

# Kirkwood–Buff Analysis of Liquid Mixtures in an Open Boundary Simulation

Debashish Mukherji,<sup>†</sup> Nico F. A. van der Vegt,<sup>‡</sup> Kurt Kremer,<sup>†</sup> and Luigi Delle Site<sup>\*,§,||</sup>

<sup>†</sup>Max-Planck Institut für Polymerforschung, Ackermannweg 10, 55128 Mainz, Germany

<sup>‡</sup>Center for Smart Interfaces, Technical University Darmstadt, Petersenstrasse 32, 64287 Darmstadt, Germany

<sup>§</sup>Institute for Mathematics, Freie Universität Berlin, Arnimallee 6, 14195 Berlin, Germany

<sup>||</sup>Max-Planck Institut für Polymerforschung, Ackermannweg 10, 55128 Mainz, Germany

**ABSTRACT:** Using the adaptive resolution (AdResS) molecular dynamics scheme, we present a new approach to calculate the thermodynamic properties of liquid mixtures in an open boundary simulation. As a test case, we simulate methanol–water mixtures. We show that Kirkwood–Buff integrals (KBI), which directly connect global thermodynamic properties to microscopic molecular distributions, can be efficiently calculated over a wide range of methanol mole fractions by choosing only a very small ( $\sim 3\%$  of total simulation domain) open boundary explicit (all atom) region and a surrounding coarse-grained reservoir that takes care of correct particle fluctuations.

## 1. INTRODUCTION

Many biophysical and biochemical processes in water are determined by interactions of dissolved, low molecular weight components or cosolvents within the hydration shells of dissolved (macro)molecules.<sup>1–4</sup> They range from small hydrophobic solutes<sup>5,6</sup> to large protein structures.<sup>7</sup> Molecular simulations of dissolved ions, osmolytes, or chemical denaturants interacting with (macro)molecules in aqueous solution are computationally expensive but may potentially contribute to advancing our understanding of physical mechanisms that control the regulation of structure, stability, and function of proteins and membranes.<sup>8–12</sup> Computational approaches to simulating these complex systems are however mostly limited to molecular simulations of middle sized systems in the NVT (constant number of particles,  $N$ ; volume,  $V$ ; and temperature,  $T$ ) or NpT (constant,  $N$ ; pressure,  $p$ ; and  $T$ ) ensembles. While these conditions are perfectly suitable in many cases, problems may arise when concentration fluctuations are large or intimately linked to the physical problem of interest. Examples include highly nonideal solution mixtures of water and cosolvents and biomolecular systems in which preferential interaction or binding of the cosolvent or water molecules to a protein surface is balanced by cosolvent/water depletion elsewhere in the simulation domain. Here, the thermodynamic condition is ill-defined away from the protein due to the closed boundary of the “small” simulation volume. This complicates a comparison with experiments conducted under (osmotic) conditions with fixed chemical potentials of the solvent components. Of course these issues can, in principle, be resolved by simulating enormously large system sizes and/or by using an alternative method to predict the Kirkwood–Buff integrals from middle sized systems.<sup>13,14</sup>

However, increasing system size is not always feasible in practice, especially when all atomistic details are to be included. Therefore, we propose to use a previously developed adaptive resolution simulation (AdResS) method,<sup>15</sup> which describes a small subvolume of a much larger system in atomistic detail, maintaining osmotic equilibrium with a surrounding reservoir of coarse grained solvent particles. We analyze the atomistic subvolume within the framework of Kirkwood–Buff (KB) theory developed for open systems. To show the validation of the approach, we use a test case of methanol–water mixtures over a wide range of methanol mole fractions and compare the results with all-atom simulations and existing experiments.

The remainder of the paper is organized as follows: In section 2, we sketch the method. We present our results in section 3, and finally we give conclusions in section 4.

## 2. METHODOLOGY

For the simulations, we use the GROMACS molecular dynamics package.<sup>16</sup> The methanol/water mixtures are simulated using the Gromos43a1 force field<sup>17</sup> for methanol and the SPC/E water model.<sup>18</sup> The  $\text{CH}_3$  group in the methanol is treated as a united atom. We consider three different methanol mole fractions of 0.250, 0.500, and 0.750, as well as pure methanol and pure water. The all-atom simulations are done in an NpT ensemble, where the pressure is controlled with a Berendsen barostat at 1 atm of pressure using a coupling time of 0.5 ps.<sup>19</sup> The methanol molecules are constrained using the LINCS algorithm. The temperature is set to 300 K using a Berendsen thermostat with a coupling time of 0.1 ps. The integration time step is set to 2 fs. Electrostatics in the all-atom simulations are treated using particle mesh ewald. AdResS simulations are performed using a modified GROMACS code.<sup>20</sup> The electrostatics for the AdResS setup is treated using a reaction field method.<sup>21</sup> The reaction field dielectric constant  $\epsilon_r$  is calculated from the all-atom simulation trajectory.<sup>22</sup>

**2.1. Kirkwood–Buff Theory (KB).** Fluctuation solution theory, derived by Kirkwood and Buff,<sup>23</sup> relates fluctuations in the grand canonical ensemble to integrals of radial distribution functions  $g_{ij}(r)$  over the volume. These “so-called” Kirkwood–Buff integrals (KBI) are related to thermodynamic properties of mixtures, including partial molar volumes, isothermal compressibility, and derivatives of chemical potentials—or solvation free energies—with respect to composition variables.<sup>23,24</sup> Previous applications of this theory include atomistic force

Received: October 6, 2011

Published: January 25, 2012

field development,<sup>25–27</sup> where force field parameters are derived by fitting the theoretical KBI values to those obtained from the experiments, molecular simulation studies of ion pairing,<sup>28,29</sup> and studies of solvation properties of biological molecules in water/cosolvent mixtures.<sup>12,30–33</sup> The KBI is defined as<sup>23,24</sup>

$$G_{ij} = V \left[ \frac{\langle N_i N_j \rangle - \langle N_i \rangle \langle N_j \rangle}{\langle N_i \rangle \langle N_j \rangle} - \frac{\delta_{ij}}{\langle N_j \rangle} \right]$$

$$= 4\pi \int_0^\infty [g_{ij}^{\mu VT}(r) - 1] r^2 dr$$

$$\approx 4\pi \int_0^r [g_{ij}^{\text{NVT}}(r') - 1] r'^2 dr' \quad (1)$$

where averages in the grand canonical ensemble are denoted by brackets  $\langle \dots \rangle$ ,  $V$  is the volume,  $N_i$  is number of particles of species  $i$  within the explicit region,  $\delta_{ij}$  is the Kronecker delta,  $g_{ij}^{\mu VT}(r)$  is the radial distribution function in the grand canonical ( $\mu VT$ ) ensemble, and  $g_{ij}^{\text{NVT}}(r)$  is the radial distribution function in the canonical (NVT) ensemble. In eq 1, we make the approximation  $g_{ij}^{\mu VT}(r) \approx g_{ij}^{\text{NVT}}(r)$ . For a very big system, this is nearly always safe, as all ensembles are equivalent in the thermodynamic limit. In practice, however, the integration of  $[g_{ij}(r) - 1]$  over the volume will hardly be feasible for systems with strong or long-range fluctuations, for instance, close to a critical point where the correlation length of concentration fluctuations becomes very large. Far away from any critical point, eq 1 is most useful for mixtures, where simulations in a grand canonical ensemble suffer from poor acceptance rates of particle insertions/deletions.<sup>34</sup> In all cases, the integration limit  $r$  in the last line of eq 1 must be chosen to be sufficiently large such that  $G_{ij}(r)$  converges to a plateau value or oscillates in a well controlled way around a mean value. Here, we take the average between  $r = 0.9$  nm and  $r = 1.5$  nm to calculate the value of  $G_{ij}$ . The resulting average is well-defined for very large NVT systems and for open boundary systems simulated with the AdResS scheme, as will be shown below.

**2.2. Adaptive Resolution (AdResS) Scheme.** In the AdResS scheme,<sup>15,35</sup> the simulation domain is divided into a small region of high resolution (e.g., atomistic) molecules and a large region of a low resolution (e.g., coarse-grained) reservoir. The molecules change their spatial resolutions (from all-atom to coarse-grained and vice versa) on the fly, during the simulation, allowing for free exchange of particles; this exchange occurs under conditions of full thermodynamic equilibrium.<sup>35</sup> The numerical as well as conceptual robustness of the method has been proved by treating challenging molecular liquids and solvation properties.<sup>20,21,36,37</sup> Here, we use the conventional AdResS scheme,<sup>15</sup> in which a spherical atomistic region is coupled to a much larger coarse-grained bath. In between, there is a “so called” hybrid region, where particles smoothly change their spatial resolution from atomistic to coarse-grained and vice versa. This transition is governed by a weighted function  $w(r) \in [0, 1]$  that interpolates the intermolecular forces between two regions.  $w(r)$  is unity for the explicit system, zero for the coarse-grained, and smoothly varies between zero and unity in the hybrid region. The interpolating force between the molecules  $\alpha$  and  $\beta$  is given by

$$\mathbf{F}_{\alpha\beta} = w(r_\alpha) w(r_\beta) \mathbf{F}_{\alpha\beta}^{\text{exp}} + [1 - w(r_\alpha) w(r_\beta)] \mathbf{F}_{\alpha\beta}^{\text{cg}} \quad (2)$$

where  $\mathbf{F}_{\alpha\beta}$  is the total intermolecular force acting between two molecules,  $\mathbf{F}_{\alpha\beta}^{\text{exp}}$  is the sum of all pairwise interactions between

atoms in the explicit region, and  $\mathbf{F}_{\alpha\beta}^{\text{cg}} = -\nabla V_{\alpha\beta}^{\text{cg}}$  with  $V_{\alpha\beta}^{\text{cg}}$  being the pairwise coarse-grained potential.  $r_\alpha$  and  $r_\beta$  are the distances of the molecular centers of mass from the center of the simulation domain. In Figure 1, we show a typical simulation

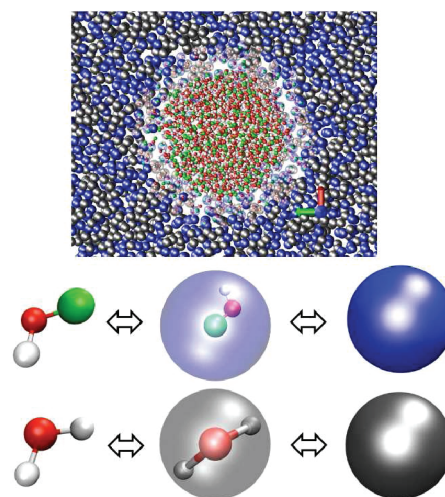


**Figure 1.** Simulation snapshot of a methanol–water system mixed at equal proportion. A cross-sectional slab is chosen to represent the simulation setup. The all-atom (explicit) region is chosen around the center of the simulation domain. To represent the hybrid region, we choose a thinner slab for the better visibility of the hybrid particles. The system consists of 10 076 water and 10 076 methanol molecules. The linear dimension of the total simulation box is  $\sim 10$  nm. The atomic representation is shown as united atom  $\text{CH}_3$  (green), O (red), H (silver), coarse-grained  $\text{CH}_3\text{OH}$  (blue), and coarse-grained  $\text{H}_2\text{O}$  (steel). (Top panel) Adaptive resolution picture of the simulation domain. The radius of the explicit region is 2 nm, and the hybrid width is 1.3 nm. The explicit region accommodates  $\sim 700$  molecules on average. (Lower panel) The coarse-grained mapping scheme shown for methanol and water.

setup of our methanol–water system for the 0.500 mol fraction of methanol. Here, the atomistic region comprises only 3% of the total simulation domain.

One of the key aspects of the AdResS scheme is that the coarse-grained region is in equilibrium with the explicit all atom regime. One way to achieve this is to systematically coarse grain our mixtures for different mole fractions to obtain appropriate coarse-grained potentials between individual beads. For this purpose, we use the iterative Boltzmann inversion (IBI) method, implemented in the VOTCA package.<sup>38</sup>

### 3. RESULTS

**3.1. All Atom Simulations.** KBIs are sensitive to severe simulation artifacts when calculated with close boundary methods. In Figure 2, we show the KBIs for four different (NpT) system sizes at a methanol mole fraction of 0.750. It is apparent that the KBI can be calculated within reasonable accuracy only for the largest system consisting of 20 152 molecules. The system size required to observe a well-behaved plateau in the KBI versus  $r$  is system specific. Methanol–water mixtures, despite the apparent miscibility of both components, show highly heterogeneous mixing characterized by extended structures in solution.<sup>39</sup> Such solution nonidealities cause anomalies in various thermodynamic excess functions and can be described within a KB framework only when large enough simulation boxes—and correspondingly long equilibration times—are used.

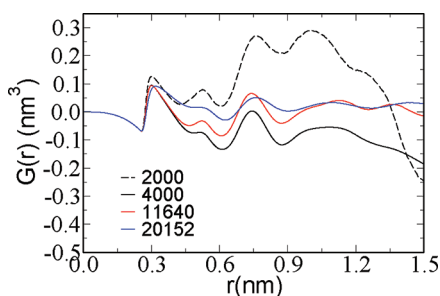


**Figure 2.** Kirkwood–Buff integral between water molecules for a mixture at a 0.750 mol fraction of methanol. Results are shown for four different system sizes (or number of molecules) and for 40 ns data.

Here, we only show the water–water KBIs for a 0.750 methanol mole fraction solution. KBIs for this system are more difficult to equilibrate than at lower methanol concentrations. The water–water KBI is furthermore larger than the methanol–methanol and methanol–water KBI, and once a limiting plateau value is observed for the water–water KBI, the remaining KBIs will automatically show plateau values as well.

**3.2. AdResS Simulations.** We perform AdResS simulations using the setup presented in Figure 1, where the total linear dimension of the simulation domain is approximately 10 nm and consists of 20 152 molecules. We choose the explicit (all-atom) region of 2 nm radius, which consists of only a 3% volume of the total simulation domain. The hybrid region is chosen to be of 1.3 nm width, and the cutoff for the interactions is 1.2 nm. We run a 20-ns-long trajectory for the mixture within the AdResS setup. Analyzing the density profile (see black curves in Figure 3),

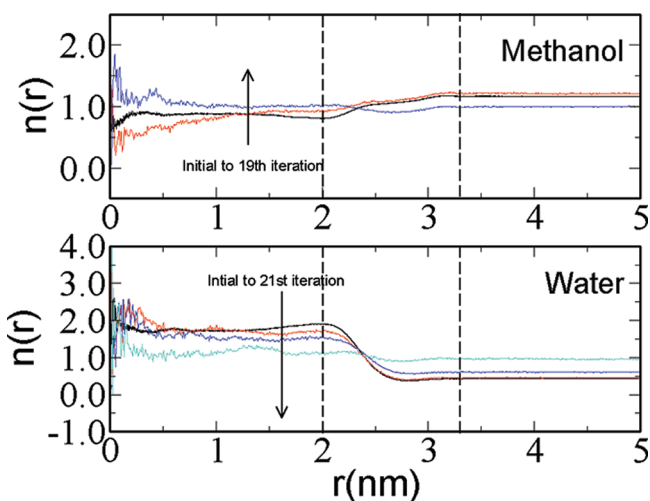


**Figure 3.** Normalized radial density profile of water and methanol for a mixture at the 0.750 mol fraction of methanol. One iteration of thermodynamic force is applied to methanol for every five iterations in water. The hybrid region is located within the two vertical lines. The number of iterations mentioned in the caption is the total iterations over which thermodynamic force is applied rather than for the individual components. The large fluctuations for the small distances are due to the poorer statistics linked to the presence of a smaller number of molecules in the corresponding shell. This is not relevant for the calculation of the thermodynamic force in the iterative procedure and in the standard simulations, where the thermodynamic force is then used.

we see that the density profile is not uniform when we just implement the scheme as given by eq 2. The nonuniform density profile is an artifact of coarse-graining procedures, since

the equation of state of the all atom and the coarse grained regime are usually not identical. Any local combination of forces thus might lead to local density fluctuations in the liquid due to a pressure balance in the whole system. Thus, a starting configuration of the system with a flat density profile will automatically evolve into a non-flat profile, once the simulation starts. It also might introduce an unphysical preferential direction for the flux of particles if the pressures in the two regions are not perfectly balanced. So, the system composition might differ inside and outside. While this so far has been taken care of by pressure correction terms,<sup>40</sup> recently it was shown how to generally avoid such complications by the introduction of a thermodynamic force in the transition regime,<sup>41,42</sup> even for the case when the (partial) pressures in the different regions of the simulation volume are of significant difference.<sup>42</sup> The thermodynamic force can be derived iteratively, starting from the hypothetical pressure profile for a totally flat density profile in the transition region. This introduction of a thermodynamic force allows one to reinterpret the AdResS method in terms of a grand canonical ensemble, where the all atom subvolume is coupled to a bath of molecules supplied by the coarse grained region.<sup>42</sup> The iteration procedure then reads<sup>42</sup>

$$f_{th}^n(r) = f_{th}^{n-1}(r) - \frac{1}{\rho^2 \kappa_T} \nabla \rho^{n-1}(r) \quad (3)$$

$\kappa_T$  is the isothermal compressibility of the system.

In the following, we demonstrate that this approach also satisfactorily applies in the case of low molecular weight mixtures, similar to simple polymer solutions.<sup>43</sup> In Figure 3, we show the flattening of the density profile for one of our samples. The iterative thermodynamic force is applied to water for five iterations, each 5-ns-long in trajectory, followed by one iteration for methanol. As shown, the flat density is achieved over whole simulation domain. We have also applied the thermodynamic force for the mixtures with different methanol mole fractions. In all cases, our approach ensures a flat density profile, though the prefactor of the thermodynamic force and the number of necessary iteration steps was found to be different.

**3.3. Calculation of KBI in AdResS.** Having ensured the thermodynamic equilibrium over the whole simulation domain, we now focus on the calculation of KBI using the AdResS scheme. In Figure 4, we show KBI for a methanol mole fraction of 0.750. It can be seen that the KBI in an AdResS simulation can easily be reproduced within reasonable accuracy. It is yet important to emphasize that the KBIs are only calculated within the explicit region that comprises only 3% of the whole simulation domain consisting of about 700 molecules, which itself would be by far too small to simulate within a closed boundary simulation (see the all atom data corresponding to the system of 2000 molecules in Figure 2), even more so when the physical properties are driven by large concentration fluctuations, such as the nonideal methanol–water mixture. Thus, we must ensure a “truly” open system that can give the correct particle fluctuations within the region of interest. We also calculated  $G_{ij}$  directly from the particle number fluctuation (see eq 1) in the explicit region. The resulting  $G_{ij}$  values are included in Figure 4 and show reasonably good agreement with the KBIs obtained by integrating the  $g_{ij}(r)$ . While we only show the results for the methanol mole fraction of 0.750 in Figure 4, we summarize the results for different methanol mole fractions in Figure 5, where we show comparative KBI values as a function of methanol mole fractions. We also want to point out that we have



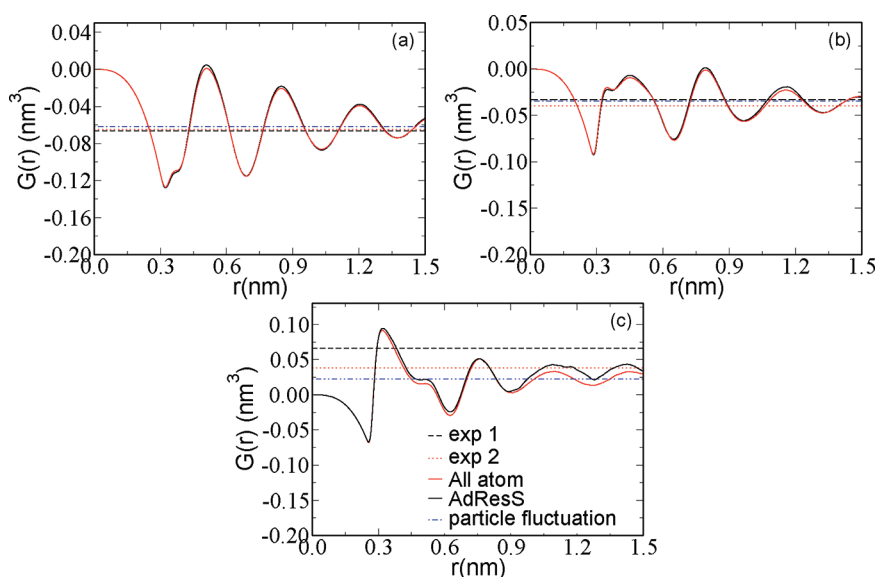


**Figure 4.** Kirkwood–Buff integral (KBI) for (a) methanol–methanol, (b) methanol–water, and (c) water–water at a methanol molar fraction of 0.750. The experimental value of KBI corresponding to the legend, exp 1, is taken from ref 24, and for exp 2 we take the value from ref 44. The KBIs for AdResS simulations and particle fluctuation are only calculated in the subvolume of the explicit region. All atom data are shown for a largest system size of 20 152 molecules.

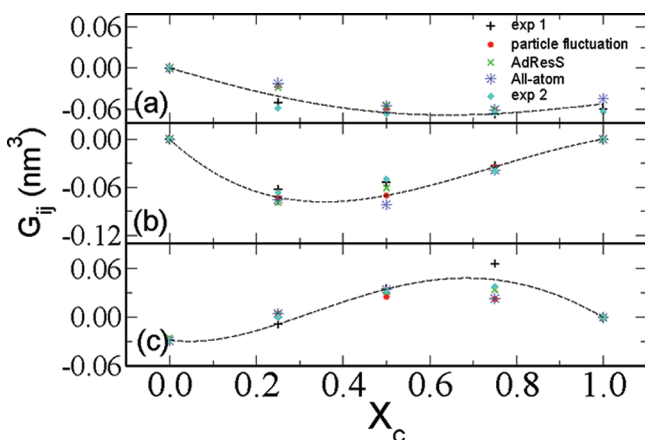


**Figure 5.** Variation of Kirkwood–Buff integral (KBI) as a function of the methanol mole fraction for (a) methanol–methanol, (b) methanol–water, and (c) water–water. The experimental value of KBI corresponding to the legend, exp 1, is taken from ref 24, and for exp 2, we take the value from ref 44. The KBIs for AdResS simulations and particle fluctuation are only calculated in the subvolume of the explicit region. Dashed lines are drawn to guide the eye.

simulated three different widths (1.5 nm, 2.0 nm, and 2.5 nm) of the explicit region. Our results indicate that the radius of 2 nm will be an optimized width for the specific system of methanol and water. Anything smaller might lead to boundary artifacts because the KBI still shows some structure at 1.5 nm, and anything more will be more computationally expensive. Therefore, our simulations were conducted for an explicit width of 2 nm. It is yet important to mention that by increasing the all-atom region and/or the hybrid width, one can expect to have significant improvement in the calculation of KBIs. However, this will require reparametrization of the thermodynamic force that intimately related to the size of the explicit and hybrid regions. While detailed analysis of this sort is beyond the scope of the present study, we want to point out that the results can be reasonably reproduced using the system parameters

used in this work. Furthermore, we also observe a speedup of up to 5 times by using AdResS for the particular systems of methanol/water mixtures, which is mostly due to the reduced effective number of particles from 60 000 in the all-atom setup to 22 000 in the AdResS set up. At a first look, this might appear to be a bit less considering the additional efforts to simulate these mixtures in AdResS. However, we do want to point out that the water in Gromacs is highly optimized, and we still see a speedup of five times with a not-so-optimized AdResS code, which is still in a development stage. Moreover, if we switch off the water optimization in Gromacs, we estimate a speedup of up to eight times.

#### 4. CONCLUSIONS

We show a new and improved approach to study Kirkwood–Buff integrals of mixtures in an open boundary simulation context using the adaptive resolution molecular dynamics scheme. For this purpose, we couple a small all-atom region to a very large coarse-grained reservoir. The coupling allows the free exchange of particles in thermodynamic equilibrium, making the all-atom region a truly open boundary system. The Kirkwood–Buff integrals of methanol–water cosolvent mixtures at various methanol mole fractions are calculated within this small all-atom region approach. Results show excellent agreement with the much larger and computationally more expensive all-atom simulations and known experiments. Additionally, we also show that particle fluctuations in the explicit region are in perfect agreement with the all-atom simulation. Our approach presents another example of the robustness of the efficient AdResS method, which can further be used to model conformational transitions of macromolecules and the chemical denaturation of proteins, driven by changes in the activity of salts and chemical denaturants.

#### AUTHOR INFORMATION

##### Corresponding Author

\*E-mail: luigi.dellesite@fu-berlin.de.

## Notes

The authors declare no competing financial interest.

## ■ ACKNOWLEDGMENTS

We thank Denis Andrienko and Christine Peter for critical reading of the manuscript. Stimulating discussions with Sebastian Fritsch, Christoph Junghans, Simon Poblete, Raffaello Potestio, and Jia-Wei Shen are gratefully acknowledged. Snapshot in this manuscript is rendered using VMD.<sup>45</sup>

## ■ REFERENCES

- (1) Zhang, Y. J.; Cremer, P. S. *Curr. Opin. Chem. Biol.* **2006**, *10*, 658–663.
- (2) Ball, P. *Chem. Rev.* **2008**, *108*, 74–108.
- (3) Kunz, W. *Specific ion effects*; World Scientific: Singapore, 2010.
- (4) Delle Site, L.; Holm, C.; van der Vegt, N. F. A. *Top. Curr. Chem.* **2012**, *307*, 251–294.
- (5) Ben-Naim, A. J. *Phys. Chem.* **1967**, *71*, 4002–4007.
- (6) van der Vegt, N. F. A.; van Gunsteren, W. F. J. *Phys. Chem. B* **2004**, *108*, 1056–1064.
- (7) Ma, L.; Pegram, L.; Record, M. T.; Cui, Q. *Biochemistry* **2010**, *49*, 1954–1962.
- (8) Kauzmann, W. *Adv. Protein Chem.* **1959**, *14*, 1–63.
- (9) Wyman, J. *Adv. Protein Chem.* **1964**, *19*, 223–286.
- (10) Dill, K. *Biochemistry* **1990**, *29*, 7133–7155.
- (11) Record, M. T.; Zhang, W. T.; Anderson, C. F. *Adv. Protein Chem.* **1998**, *51*, 281–353.
- (12) Hess, B.; van der Vegt, N. F. A. *Proc. Natl. Acad. Sci.* **2009**, *106*, 13296–13300.
- (13) Wedberg, R.; O'Connell, J. P.; Peters, G. H.; Abildskov, J. *J. Chem. Phys.* **2011**, *135*, 084113–9.
- (14) Schnell, S. K.; Liu, X.; Simon, J.; Bardow, A.; Bedeaux, D.; Vlugt, T. J. H.; Kjelstrup, S. J. *Phys. Chem. B* **2011**, *115*, 10911–10918.
- (15) Praprotnik, M.; Delle Site, L.; Kremer, K. *J. Chem. Phys.* **2005**, *123*, 224106–14.
- (16) Lindahl, E.; Hess, B.; van der Spoel, D. *J. Mol. Mod.* **2001**, *7*, 306–317.
- (17) van Gunsteren, W. F.; Billeter, S. R.; Eising, A. A.; Hünenberger, P. H.; Krüger, P.; Mark, A. E.; Scott, W. R. P.; Tironi, I. G. *Gromos43a1*; Hochschulverlag AG an der ETH Zürich: Zürich, Switzerland, 1996.
- (18) Berendsen, H. J. C.; Grigera, J. R.; Straatsma, T. P. *J. Phys. Chem.* **1987**, *91*, 6269–6271.
- (19) Berendsen, H. J. C.; Postma, J. P. M.; van Gunsteren, W. F.; DiNola, A.; Haak, J. R. *J. Chem. Phys.* **1984**, *81*, 3684–3690.
- (20) Fritsch, S.; Junghans, C.; Kremer, K. *J. Chem. Theory Comput.* **2012**, DOI: 10.1021/ct200706f.
- (21) Praprotnik, M.; Matysiak, S.; Delle Site, L.; Kremer, K.; Clementi, C. *J. Phys. Condens. Mater.* **2007**, *19*, 292201–10.
- (22) Reaction field dielectric constants are taken from PME treated all-atom simulations. The values are  $\epsilon_r = 67.5998$  for pure water, 52.4122 for 25% methanol, 44.5407 for 50% methanol, 36.4963 for 75% methanol, and 12.5426 for pure methanol.
- (23) Kirkwood, J. G.; Buff, F. P. *J. Chem. Phys.* **1951**, *19*, 774–777.
- (24) Ben-Naim, A. *Molecular Theory of Solutions*; Oxford University Press: New York, 2006.
- (25) Weerasinghe, S.; Smith, P. E. *J. Phys. Chem. B* **2005**, *109*, 15080–15086.
- (26) Lee, M. E.; van der Vegt, N. F. A. *J. Chem. Phys.* **2005**, *122*, 114509–13.
- (27) Gee, M. B.; Cox, N. R.; Jiao, Y. F.; Benteitis, N.; Weerasinghe, S.; Smith, P. E. *J. Chem. Theory Comput.* **2011**, *7*, 1369–1380.
- (28) Kalcher, I.; Dzubiella, J. *J. Chem. Phys.* **2009**, *130*, 134507–12.
- (29) Ganguly, P.; Schravendijk, P.; Hess, B.; van der Vegt, N. F. A. *J. Phys. Chem. B* **2011**, *115*, 3734–3739.
- (30) Ruckenstein, E.; Shulgin, I. L. *Adv. Colloid Interface Sci.* **2006**, *123*, 97–103.
- (31) Shulgin, I. L.; Ruckenstein, E. *Biophys. J.* **2006**, *90*, 704–707.
- (32) Pierce, V.; Kang, M.; Aburi, M.; Weerasinghe, S.; Smith, P. E. *Cell Biochem. Biophys.* **2008**, *50*, 1–22.
- (33) Algaer, E. A.; van der Vegt, N. F. A. *J. Phys. Chem. B* **2011**, *115*, 13781–13787.
- (34) Frenkel, D.; Smit, B. *Understanding Molecular Simulations*; Academic Press: New York, 2002.
- (35) Praprotnik, M.; Delle Site, L.; Kremer, K. *Annu. Rev. Phys. Chem.* **2008**, *59*, 545–571.
- (36) Lambeth, B. P. Jr.; Junghans, C.; Kremer, K.; Clementi, C.; Delle Site, L. *J. Chem. Phys.* **2010**, *133*, 221101–4.
- (37) Poma, A. B.; Delle Site, L. *Phys. Rev. Lett.* **2010**, *104*, 250201–4.
- (38) Rühle, V.; Junghans, C.; Lukyanov, A.; Kremer, K.; Andrienko, D. *J. Chem. Theory Comput.* **2009**, *5*, 3211–3223.
- (39) Dougan, L.; Bates, S. P.; Hargreaves, R.; Fox, J. P.; Crain, J.; Finney, J. L.; Reat, V.; Soper, A. K. *J. Chem. Phys.* **2004**, *121*, 6456–6462.
- (40) Wang, H.; Junghans, C.; Kremer, K. *Eur. Phys. J. E* **2009**, *28*, 221–9.
- (41) Poblete, S.; Praprotnik, M.; Kremer, K.; Delle Site, L. *J. Chem. Phys.* **2010**, *132*, 114101–7.
- (42) Fritsch, S.; Poblete, S.; Junghans, C.; Delle Site, L.; Ciccotti, G.; Kremer, K. arXiv:cond-mat/1112.3151.
- (43) Praprotnik, M.; Poblete, S.; Kremer, K. *J. Stat. Phys.* **2011**, *145*, 946–966.
- (44) Marcus, Y. *Phys. Chem. Chem. Phys.* **1999**, *1*, 2975–2983.
- (45) Humphrey, W.; Dalke, A.; Schulten, K. *J. Mol. Graphics* **1996**, *14*, 33–38.